J. Phys. Chem. A **2006,** *110,* 9549−9554

Dynamic Solvation in Imidazolium-Based Ionic Liquids on Short Time Scales

Lindsay Sanders Headley, Prasun Mukherjee, Jared L. Anderson, Rongfang Ding,
Mintu Halder, Daniel W. Armstrong, Xueyu Song, and Jacob W. Petrich*

Department of Chemistry, Iowa State University, Ames, Iowa 50011

Received: February 1, 2006; In Final Form: May 18, 2006

Steady-state and time-resolved Stokes shift data for the probe coumarin 153 in two imidazoles, six imidazolium-based ionic liquids, and several other solvents are presented. These results are consistent with our original suggestion (*J. Phys. Chem. B* **2004**, *108*, 10245−10255) that initial solvation is dominated by the organic moiety of the ionic liquid, and they show that for the imidazole-based liquids initial solvation is in all cases very rapid. Solvation by methylimidazole and butylimidazole is complete in 100 ps, and all of the imidazolium ionic liquids demonstrate similarly rapid initial solvation. Owing to the importance of determining the amount of initial solvation that is missed in a given experiment with finite time resolution, we discuss a method of estimating the intramolecular contribution to the reorganization energy. This method yields 2068 cm^{-1} and is compared with an alternative method.

Introduction

Room temperature ionic liquids (RTILs) are comprised of an organic cation and an inorganic anion. They have been used as novel solvent systems for organic synthesis,[1−14] liquid−liquid extraction,[15−17] and electrochemical studies[18] and as ultralow volatility liquid matrixes for matrix-assisted laser desorption/ionization (MALDI) mass spectrometry.[19] RTILs have many properties that make their applications in chemical systems attractive. Some are immiscible with both water and nonpolar organic solvents. They are stable to temperatures in excess of 300 °C, but they have negligible vapor pressures, thus making them “green” solvents by reducing environmental levels of volatile organic carbons. Their viscosities can easily be varied by changing their cationic or anionic constituents. Their growing utility requires a detailed and fundamental understanding of their behavior.

Early treatments of solvation by ionic fluids were provided by Huppert and co-workers using molten salts[20,21] and by Maroncelli and co-workers using nonaqueous solutions of dissolved ions.[22] More recently, solvation by RTILs has been studied by fluorescence techniques by Karmakar and Samanta[23−25] and by Maroncelli and co-workers.[26−31] Karmakar and Samanta have argued that the solvation dynamics is biphasic, with a short component corresponding to diffusional motion of the anion and a long component corresponding to the collective motion of the anion and the cation. Maroncelli and co-workers, however, have insisted on the nonexponential nature of the solvation dynamics and on the glassiness of the RTILs. Several groups[32−37] have used the optical Kerr effect to study ionic liquids. Finally, Weingärtner and co-workers[38,39] and Richert and co-workers[40] have investigated the dielectric relaxation of ionic liquids.

Previously, we suggested that the organic cation determined the early-time solvation behavior of these materials.[41] This conclusion was based on a comparison of the behavior of an ionic liquid based on an imidazolium cation and the uncharged organic counterpart, butylimidazole. Castner and co-workers[37] have subsequently performed similar studies comparing an ionic liquid with its isoelectronic neutral binary counterpart using femtosecond optical Kerr effect spectroscopy.

Here, we present steady-state and time-resolved Stokes shift data for the probe coumarin 153 in two imidazoles, six imidazolium-based ionic liquids, and several other solvents (Figure 1 and Table 1). These results are consistent with our original suggestion, and they show that for the imidazole-based liquids initial solvation is in all cases very rapid.

Since there is always some finite time resolution associated with the measurement of a dynamic Stokes shift, it is important to know how much of the Stokes shift has been missed in the measurement, or, alternatively, what fraction of the total solvation has been completed at a given time. Fee and Maroncelli[42] have discussed this question at length and have indicated a method of estimating a “zero-time” emission spectrum, which reflects a vibrationally equilibrated emissive state that has not yet experienced any Stokes shift resulting from solvent motion. We propose a method for estimating the intramolecular contribution to the reorganization energy, which is an alternative but equivalent means of obtaining the same information.

Materials and Methods

Ionic Liquids. All of the ionic liquids are prepared via their chloride salts. 1-Methylimidazolium chloride, 1-butylimidazolium chloride, and 1,2-dimethylimidazolium chloride were synthesized by adding a 1:1 molar ratio of hydrochloric acid dropwise to a round-bottom flask containing 1-methylimidazole, 1-butylimidazole, or 1,2-dimethylimidazole in ∼100 mL of 2-propanol. After stirring for 2 h at room temperature, the solvent was removed using rotary evaporation. The bis[(trifluoromethyl)-sulfonyl]imide (NTf_2^-) ionic liquids were synthesized by dissolving the chloride ionic liquids in 100−150 mL of water. One molar equivalent of lithium trifluromethanesulfonimide was dissolved in 50 mL of water and added to the chloride salt. After stirring for 2 h, the lower ionic liquid layer was washed with at least three 30 mL portions of water. A silver nitrate test was used to verify the removal of any excess chloride salt. The resulting ionic liquids were dried overnight in a vacuum desiccator under P_2O_5. Triethylammo-

---

* To whom correspondence should be addressed.

10.1021/jp0606964 CCC: $33.50

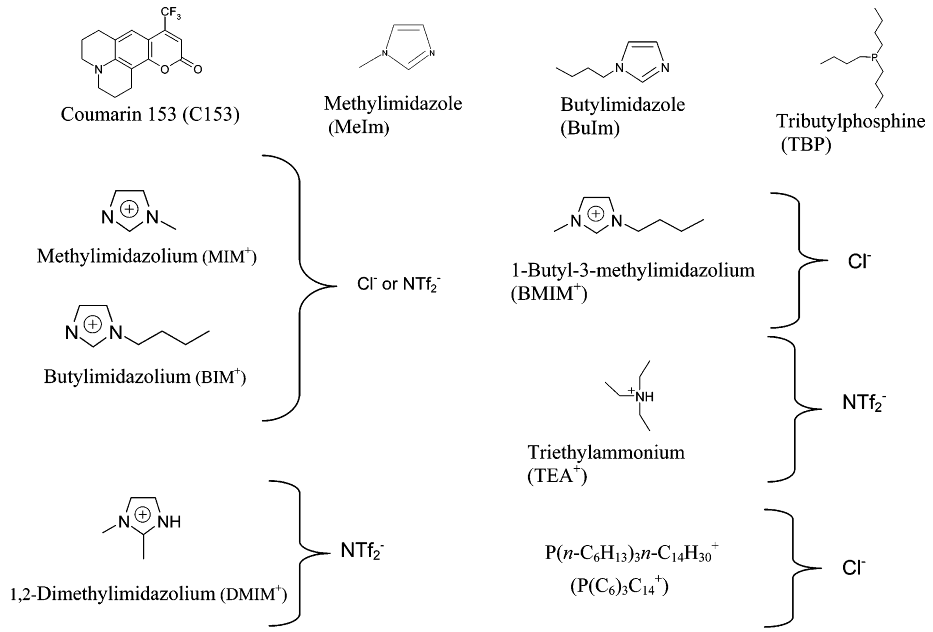

Figure 1. Structures of the solvation probe, coumarin 153, along with methylimidazole (MeIm), butylimidazole (BuIm), and tributylphosphine (TBP). Structures are also provided for the RTILs studied: the methylimidazolium cation [MIM^+], the butylimidazolium cation [BIM^+], the 1,2-dimethylimidazolium cation [$DMIM^+$], the 1-butyl-3-methylimidazolium cation [$BMIM^+$], the triethylammonium cation [TEA^+], and the corresponding anions. The phosphonium ionic liquid, [$P(C_6)_3C_{14}^+$][Cl^-], was investigated by Maroncelli and co-workers.[29]

TABLE 1: Spectral Characteristics of Coumarin 153 in Various RTILs

RTIL[a]	η (cP)	$\langle\nu\rangle_{abs}$[b] (cm^{-1})	$\langle\nu\rangle_{em}$[b] (cm^{-1})	$\lambda_{“t=0”}$[c] (cm^{-1})	λ[c] (cm^{-1})	f_{100ps}[d]	$\langle\tau\rangle_{SR}$ (ns)
MeIm	1.76 ± 0.02[e]	24 000	18 330	1483	2923	1.0	<0.02
TBP	2.18 ± 0.01	25 100	21 030	2114	2239	1.0	0.080
BuIm	3.50 ± 0.06[e]	24 040	18 700	1629	2919	0.57	0.10
MIM^+Cl^-	8.7 ± 0.2[e]	23 450	17 430	1782	2620	1.0	0.082
$TEA^+NTf_2^-$ [f]	56.7 ± 0.2	23 690	17 920	1908	2744	0.77	0.17
$BIM^+NTf_2^-$	90.03 ± 1.5	23 210	18 070	1867	2706	0.65	0.20
$DMIM^+NTf_2^-$	117.3 ± 0.9	22 190	18 020	2021	2471	0.30	0.71
$P(C_6)_3C_{14}^+Cl^-$ [g]	230[h]					0	6.7[g]
$BMIM^+Cl^-$ (70 °C)	334[i]	23 540	18 090	1910	2798	0.21	0.59
$MIM^+NTf_2^-$	776.3 ± 3.1	22 980	18 190	1952	2598	0.64	0.42
BIM^+Cl^-	1130 ± 20	22 940	18 270	2052	2606	0.39	0.76
$BMIM^+Cl^-$ (30 °C)	11 000[i]	23 490	18 570	1842	2557	0.36	1.3

[a] For abbreviations, see the caption of Figure 1. Unless indicated, the parameters reported are for 20 °C. [b] $\langle\nu\rangle = (\int_0^\infty \nu\, I(\nu)\, d\nu / \int_0^\infty I(\nu)\, d\nu)$, computed using 70% of the emission and excitation spectra in order to exclude the contributions from absorption to states higher than S_1 in energy. [c] Computed from eq 1. [d] There are instances where the fractional solvation does not track the viscosity as expected. We attribute this to our definition of “100 ps”, as indicated in the Materials and Methods section. [e] These viscosities were kindly measured for us by personnel in Professor E. W. Castner Jr.’s laboratory before we had acquired our own viscometer. [f] [TEA^+][NTf_2^-] is included for completeness. We hoped to compare it with the chloride salt, which proved impossible, since the latter melts at 261 °C. [g] From ref 29, at 58 °C. [h] From ref 61. [i] From ref 62.

nium chloride was purchased from Alfa Aesar. Triethylammonium NTf_2^- was made using the same anion exchange as described above. The role of water on the physical properties of ionic liquids is well-known, and an excellent study is provided by Bright and co-workers.[43] This work indicates that the solvation probe, PRODAN, is highly sensitive to water content. On the other hand, Ito et al.[28] have shown that coumarin 153 is fortuitously insensitive to the presence of water, most likely owing to its hydrophobic character.

Viscosity measurements for tributylphosphine (TBP), [TEA^+][NTf_2^-], [BIM^+][NTf_2^-], [$DMIM^+$][NTf_2^-], [MIM^+][NTf_2^-], and [BIM^+][Cl^-] were taken with a ViscoLab 4000 piston-style viscometer from Cambridge Applied Systems. The digital readout provided the viscosity and interior temperature along with measurement errors. The viscosity of the TBP was measured in a glovebag under argon. Measurements were taken at various pressures to ensure that the viscosity reading was not significantly affected by the positive pressure inside the glovebag. Viscosity measurements for methylimidazole (MeIm), butylimidazole (BuIm), and [MIM^+][Cl^-] were provided by Professor E. W. Castner, Jr. (Rutgers) using a Cambridge Applied System model ViscoLab 4100 automated viscometer (SPL480 sensor with thermal jacket). Temperature was controlled with a Lauda Refrigerating Circulator model RMT-6, accurate to 0.1 K.

Steady-State Measurements. Steady-state excitation and emission spectra were recorded with a SPEX Fluoromax instrument with a 4 nm band-pass and were corrected for detector response. A 1 cm path length quartz cuvette was used for the measurements. During spectroscopic measurements, the quartz cuvettes were kept tightly sealed to prevent moisture from being absorbed by the ionic liquids. The steady-state spectra can be used to compute the reorganization energy, λ, by means of[44]

$$\lambda = \hbar \frac{\int_0^\infty d\nu [\sigma_a(\nu) - \sigma_f(\nu)]\nu}{\int_0^\infty d\nu [\sigma_a(\nu) + \sigma_f(\nu)]} \tag{1}$$

The $\sigma_{a,f}$ are the absorption (or excitation) and emission spectral line shapes, respectively. The reorganization energy is widely

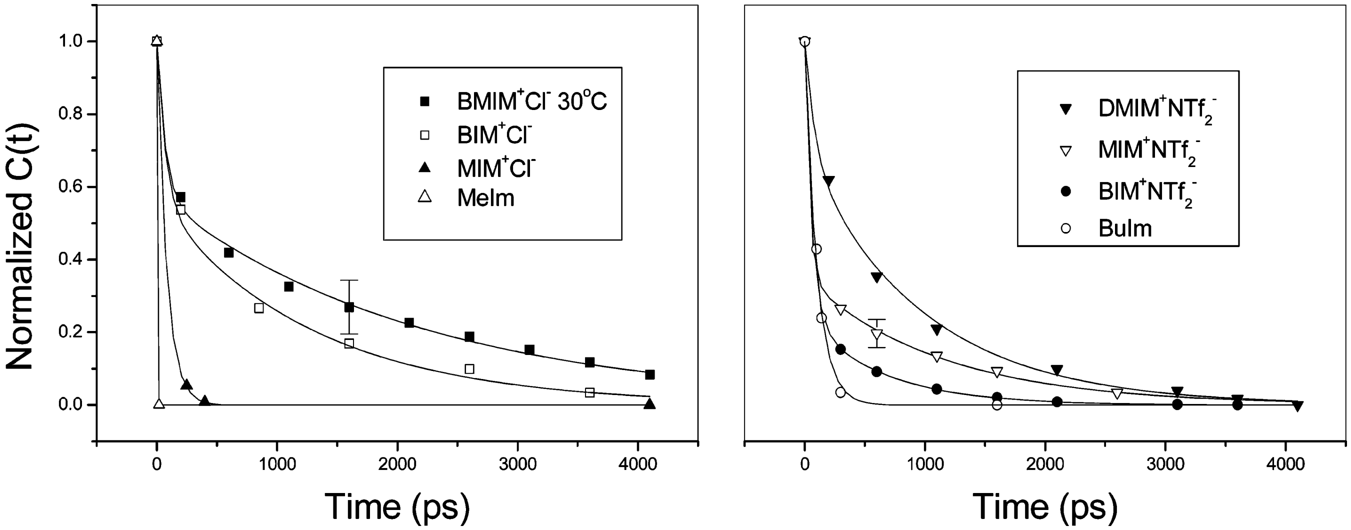

Figure 2. Solvation correlation functions, *C*(*t*), for the imidazole-based solvents. Two exponentials were sufficient to describe the data. A representative error bar is shown for [BMIM$^+$][Cl$^-$] and [MIM$^+$][NTf$_2$$^-$].

used as a measure of the strength of interactions between a chromophore and its surrounding dielectric media in solvation dynamics studies. It is usually taken as half of the Stokes shift. This estimate is accurate if the excitation and emission spectra are Gaussian, but it becomes unreliable if they are not.

Time-Resolved Measurements. The laser source for the time-correlated single-photon counting measurements was a homemade mode-locked Ti-sapphire laser, tunable from 780 to 900 nm with a repetition rate of 82 MHz. The fundamental from the Ti-sapphire oscillator was modulated by a Pockels cell (model 350-160, Conoptics Inc) to reduce the repetition rate to about 8.8 MHz and was subsequently frequency doubled by focusing tightly into a 0.4 mm BBO crystal. The resulting blue light, which had a central wavelength of 425 nm, provided the excitation source. The fluorescence decays were collected at the magic angle (polarization of 54.7° with respect to the vertical). Emission was collected through a single monochromator (ISA H10) fitted with a slit having an 8 nm band-pass. A half-wave plate before a vertical polarizer ensured the polarization of the excitation light. The instrument response function of the apparatus had a full width at half-maximum (fwhm) of $\leq$100 ps. A 1 cm path length quartz cuvette was used for all of the time-resolved measurements. To construct the time-resolved spectra, a series of decays ($\sim$3000 counts in the peak channel) were collected over as much of the fluorescence spectrum as possible, typically from 470 to 610 nm at 10 nm intervals. They were fit to a maximum of three exponentials. Transient spectra were reconstructed from these fits by normalizing to the steady-state spectra:

$$S(\lambda,t) = D(\lambda,t)\frac{S_0(\lambda)}{\int_0^\infty D(\lambda,t)} \tag{2}$$

$D(\lambda,t)$ is the wavelength-resolved fluorescence decay, and $S_0(\lambda)$ is the steady-state emission intensity at a given wavelength. We have employed the traditional approach of fitting the time-resolved spectra to a log-normal function, from which we extract the peak frequency, $\nu(t)$, as a function of time.

The solvation dynamics were described by the normalized correlation function:

$$C(t) = \frac{\nu(t) - \nu(\infty)}{\nu(\text{“}t{=}0\text{”}) - \nu(\infty)} \tag{3}$$

$\nu(\text{“}t{=}0\text{”})$ is the frequency at zero time, calculated using the method described by Fee and Maroncelli.[42] $\nu(\infty)$ is the frequency at “infinite time”, the maximum of the steady-state fluorescence spectrum. $\nu(t)$ is determined by taking the maximum from the log-normal fits as the emission maximum. In most of the cases, however, the spectra are broad, so there is some uncertainty in the exact position of the emission maxima. Thus, we have considered the range of the raw data points in the neighborhood of the peak to estimate an error for the maximum obtained from the log-normal fit. Depending on the width of the spectrum (i.e., zero-time, steady-state, or time-resolved emission spectrum), we have determined the typical uncertainties as follows: zero-time $\sim$ steady-state ($\sim \pm100$ cm^{-1}) < time-resolved emission ($\sim \pm200$ cm^{-1}). We use these uncertainties to compute error bars for the computed *C*(*t*). Some representative error bars are given in Figure 2. Some representative steady-state, zero-time, and 100 ps spectra are presented in Figure 3.

Finally, in generating *C*(*t*), the first point was obtained from the zero-time spectrum. The second point was taken at the maximum of the instrument response function, which, having a full width at half-maximum of $\leq$100 ps, was taken to be $\sim$100 ps. Fractional solvation at 100 ps was calculated using $f(t{=}100 \text{ ps}) = 1 - C(t{=}100 \text{ ps})$.

Results and Discussion

Solvation by Imidazoles and Imidazoliums. Figure 2 presents the experimentally obtained solvation relaxation correlation functions for two imidazoles and several imidazolium-based ionic liquids. There is a very rapid early phase of solvation in all of these solvents, which is consistent with our previous suggestion that the organic cation, at least for imidazolium-based ionic liquids, dominates the early-time solvation behavior[41] (Table 1). Furthermore, it is reasonable to assume that symmetrical nonpolar inorganic anions such as Cl$^-$, BF$_4$$^-$, and PF$_6$$^-$ play a negligible role in the solvation of the coumarin probe. We are cautious, however, to extend this conclusion to the NTf$_2$$^-$ anion, which is polar, polarizable, large, and flexible.[35] The data presented in Figure 2 and Table 1 are not sufficient to draw a conclusion concerning the role of this anion. Table 1 also indicates that the solvation dynamics correlate well with viscosity, and Figure 4 compares the average solvation time against the solvent viscosity on a logarithmic scale.

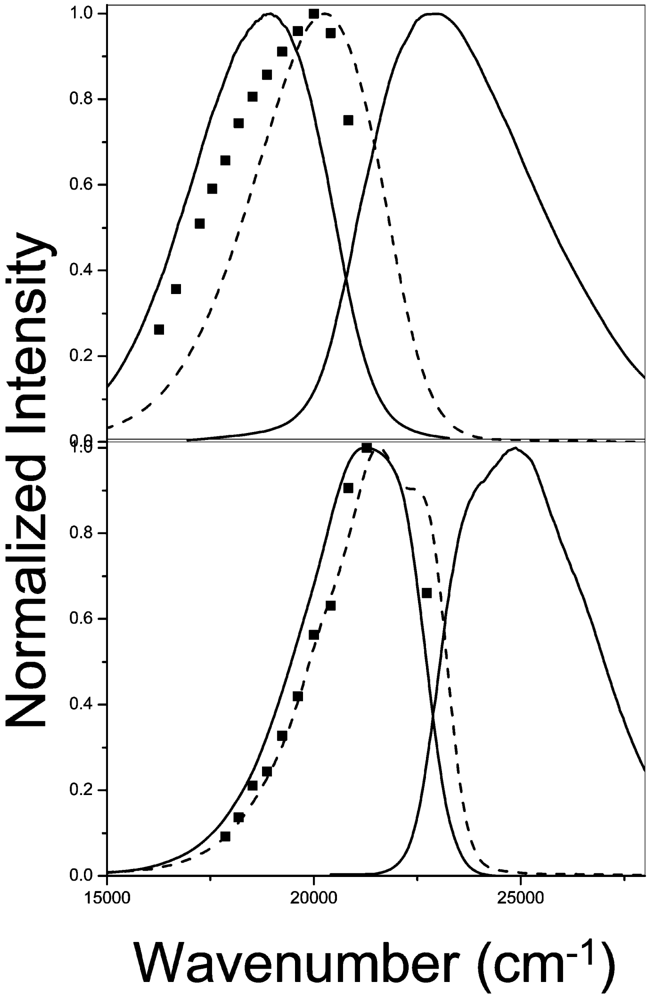

Figure 3. Fluorescence emission and excitation curves for $BMIM^+Cl^-$ at 30 °C (top) and TBP (bottom). The solid lines are the steady-state data, the dashed lines are the calculated zero-time emission curves, and the scattered dots are the time-resolved emission spectra at our instrument's shortest collection time. The steady-state excitation wavelengths were 420 nm for $[BMIM^+][Cl^-]$ and 400 nm for TBP. The emission monochromator was set to 600 nm for $[BMIM^+][Cl^-]$ and 500 nm for the TBP.

Maroncelli and co-workers have used such a linear correlation to argue for translational ionic motion.[30] While it is reasonable that there is indeed such translational motion in ionic liquids, we do not find the linearity of a log−log plot as compelling evidence for the role of such motion in the solvation process.

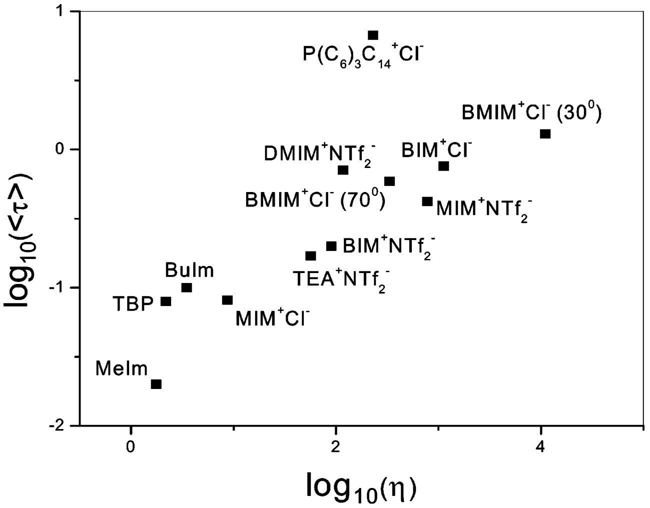

Figure 4. Log−log plot of the average solvation times against the viscosities of the ionic liquids and corresponding organic solvents. There is a good correlation between the two properties. The phosphonium solvent lies off the line described by the imidazoliums. It is expected that different solvent types yield different slopes on such plots.[30]

Phosphine and Phosphonium. Maroncelli and co-workers[29] have studied the solvation of several nonpolarizable, long-chain ionic liquids, in particular $[N(n\text{-}C_4H_9)_3CH_3{}^+][Tf_2N^-]$ and $[P(C_6)_3C_{14}{}^+][Cl^-]$. For these solvents, in contrast to the imidazolium-based liquids, there is no ultrafast solvation response and consequently the entire solvation response can be measured. On the basis of our earlier comparison of $[BMIM^+][\ PF_6{}^-]$ and butylimidazole, we undertook a study of tributylphosphine (TBP) in order to compare its behavior with that of $P(C_6)_3C_{14}{}^+$ (Figure 1). We anticipated that the nonpolarizable butyl side chains of TBP would give rise to slow solvation dynamics. Notwithstanding its small viscosity, 2.2 cP, the fractional solvation at 100 ps of 1.0 and the average solvation time of 0.08 ns seem surprising. The steady-state reorganization energy of TBP is, however, 2240 cm^{-1} as opposed to 2068 or 1870 ± 185 cm^{-1}, which one obtains from nonpolar solvents or from zero-time spectra of initially "unsolvated" chromophores (see below). TBP behaves more like a polar molecule than one would expect and is consequently not a good model for the organic counterpart of $P(C_6)_3C_{14}{}^+$.

Determination of the Intramolecular Contribution to the Reorganization Energy, λ. To estimate the intramolecular contribution to the reorganization energy of coumarin 153 (C153) and to establish a classical model for C153 in studies of solvation dynamics (that is, a rigid solute molecule with a charge distribution change), we performed a regression analysis of C153 in 13 solvents with various dielectric constants.[45] The initial charge distribution change was estimated from a semiempirical quantum chemistry calculation.[46,47] The total experimental reorganization energy is estimated from the emission and excitation spectral line shapes (eq 1). The solvent contribution to the reorganization energy is calculated from the charge distribution change and the solvent static and optical dielectric constants and a realistic molecular surface and charge distribution for C153 using methods described in detail elsewhere.[44,47−54] That is, the reorganization energy, λ, is calculated as the difference between the solvation energy of C153 with the static dielectric constant of the solvent and the solvation energy of C153 with the optical dielectric constant of the solvent.

The reorganization energy, λ, is related to the solvation correlation function, $C(t)$, and to the solvation spectral density, $\rho_{\mathrm{sol}}(\omega)$, as follows:

$$C(t) = \frac{\hbar}{\lambda}\int_0^\infty \mathrm{d}\omega\ \omega\ \rho_{\mathrm{sol}}(\omega)\cos(\omega t) \tag{4}$$

and

$$\lambda = \hbar\int_0^\infty \mathrm{d}\omega\ \omega\ \rho_{\mathrm{sol}}(\omega) \tag{5}$$

where

$$\rho_{\mathrm{sol}}(\omega) = \frac{\Delta E''(\omega)}{\omega} \tag{6}$$

and $\Delta E''(\omega)$ is the imaginary part of the solvation energy, which may be computed from the frequency-dependent dielectric susceptibility of the pure solvent, the region occupied by the solute, and the charge distribution of the solute, as noted above.

TABLE 2: Solvent Reorganization Energies (cm^{-1}) for Coumarin 153

solvent	ϵ_0	$\mathbf{n}_D$	λ_{exptl}	λ_{calcd}
acetonitrile	35.94	1.433	2845	1049
dimethylformamide	36.71	1.431	2860	1053
dimethyl sulfoxide	46.45	1.479	2920	1008
acetone	20.56	1.359	2785	1095
butyronitrile	20.7	1.384	2875	1060
tetrahydrofuran	7.58	1.4035	2645	815
dichloromethane	8.93	1.424	2520	837
chloroform	4.81	1.444	2410	577
hexane	2.0	1.375	2100	0
pentane	1.8	1.34	2115	0
cyclohexane	2.0	1.41	2090	0
heptane	1.9	1.38	2070	0
octane	2.0	1.40	2020	0

A linear regression analysis between the calculated λ and the total experimental λ yields information on both the intramolecular reorganization energy contribution and the charge distribution of the solute used in the calculation described above (Table 2 and Figure 5). The plot displayed in Figure 5 yields an intercept of 2068 cm^{-1}, which is the intramolecular contribution of λ. The plot should yield a slope of 1, but in fact, the slope is 0.72. Assuming that the discrepancy arises entirely from the charge distribution of the solute, we thus rescale the charge distribution change by a factor of 1.18 (i.e., $1/(0.72)^{1/2}$, because the solvation energy is proportional to the charges squared). This procedure consequently provides an improved charge distribution for the solute.

In principle, the intramolecular contribution to λ can be obtained by measurement of the gas phase spectra. Ernsting and co-workers have presented such measurements for coumarin 153 at 383 K.[55] Computation of λ from their gas phase data yields 2610 cm^{-1}, which is considerably in excess of the value we measure in nonpolar solvents, suggesting that the coumarin in the gas phase measurement may have been complexed to solvent molecules or other coumarin molecules. In our previous work, we used the above analysis to define the fractional solvation, $f(t)$, in terms of reorganization energies.[41] Now that we have calculated the zero-time values and incorporated them into the solvation correlation function, the fractional solvation may be computed at any time. Values of $f(t=100\text{ ps})$ are given in Table 1. Finally, if the above estimate of intramolecular reorganization energy is reasonable, we can use the dielectric constant of ionic liquids measured by Weingärtner and co-workers[39] to estimate the reorganization energy of ionic liquids. For example, 1-butyl-3-methylimidazolium tetrafluoroborate has a static dielectric constant of 11.7; our theoretical estimation of the reorganization energy yields 2879 cm^{-1}. The experimental measurements give 2717 cm^{-1}; therefore, the C153 model we use appears to be appropriate for studies of solvation dynamics.

Finally, we comment on the difference in the intramolecular contribution to λ obtained from our method and that obtained from the zero-time spectra using the method of Fee and Maroncelli.[42] Namely, our method yields 2068 cm^{-1}; the zero-time method yields a range of values from 1483 to 2114 cm^{-1} corresponding to an average of 1870 ± 185 cm^{-1}. There are two major differences in the approaches. The crucial elements of the construction of the zero-time spectrum are the fluorescence and the absorption spectra of the probe in a nonpolar solvent. A Gaussian distribution of frequency shifts is convoluted with the spectra obtained in nonpolar solvents in order to produce the spectra in polar solvents. Since this convolution does not in all cases produce a perfect reproduction of the spectrum in polar solvents, the computed λ value will also be affected. Another physical reason for this difference may be that it is possible that the reference nonpolar fluorescence spectrum does not originate from a completely relaxed S_1 state: the separation of intramolecular and intermolecular solvation is a fundamental assumption of the zero-time method. On the other hand, the method we employ uses a model for the probe that cannot solvate itself; that is, the model has no intramolecular degrees of freedom. Consequently, all solvation that is calculated is only from the solvent contribution.

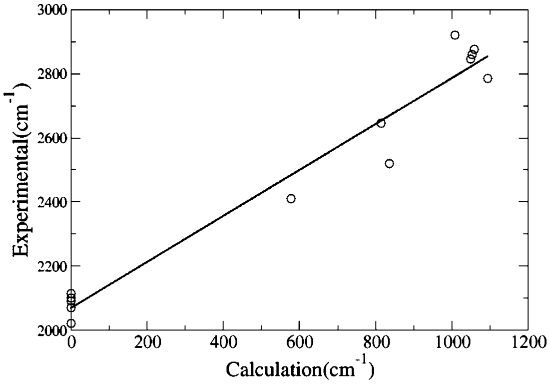

Figure 5. Plot of the reorganization energy obtained from eq 1 against that obtained from calculations. The intercept, 2068 cm^{-1}, provides the intramolecular contribution of the reorganization energy for coumarin 153.

Conclusions

The picture we originally put forward for solvation by ionic liquids was that the organic cation determined the early-time solvation behavior of these materials.[41] This conclusion was based on a comparison of the behavior of an ionic liquid based on an imidazolium cation and the uncharged organic counterpart, butylimidazole. In other words, because the organic cation carries most of the permanent dipole moment, is more polarizable, and is nearer to the solute, it seems reasonable that it contributes the most to early-time solvation events. The additional solvation data for the imidazoles and the imidazolium ionic liquids presented here are consistent with this idea. Solvation by methylimidazole and butylimidazole is complete in 100 ps, and all of the imidazolium ionic liquids demonstrate similarly rapid initial solvation. Also consistent with this idea is that Maroncelli and co-workers[29] observe no ultrafast solvation component in long-chain, nonpolar ionic liquids such as $[N(n\text{-}C_4H_9)_3CH_3^+][NTf_2^-]$ and $[P(C_6)_3C_{14}^+][Cl^-]$. We still do not completely understand, however, the rapid solvation afforded by the uncharged neutral, TBP. It is most likely at least partially attributable to its low viscosity and to the fact that it is expected to be more polar than its ionic liquid counterpart. $P(C_6)_3C_{14}^+$ can be thought of as having its positive charge spherically distributed about it, while TBP, having only three alkyl groups, assumes a pyramidal configuration and can be thought of as being a polar molecule.

Several theoretical investigations have been undertaken of ionic liquids.[56-59] In a recent computer simulation, Shim et al.[57] place a dipolar excitation on a model diatomic solute in a RTIL. They observe a fast initial relaxation and suggest that it arises from translations of the anions. Given the small size of the model solute and the large changes in net charge, the motions of the resulting concentrated anionic charges may dominate the relaxation. In the experimental solvation dynamics studies of organic dye molecules such as coumarin 153 (C153) in RTILs, the charge distribution change is smeared across the whole probe molecule, which is most likely well solvated by the bulky organic cations given the hydrophobic nature of C153 in the ground state. This also suggests, therefore, that the most possible scenario is that the cation motions dominate the contribution of the initial fast relaxation upon excitation. To elucidate the nature of the fast relaxations, a realistic model of C153 in RTILs will be needed. Znamenskiy and Kobrak have recently performed molecular dynamics simulations of the dye betaine-30 in [BMIM$^+$][PF$_6^-$].[58] They obtained radial distribution functions indicating the proximity of the 1-butyl-3-methylimidazolium ring to the dye, which is consistent with our experimental observations for coumarin 153. The solvation relaxation is argued to arise from the translation and diffusional motion of ions.

Simulations by Kobrak and Znamenskiy[59] have also indicated collective cation−anion motion on subpicosecond time scales, which again argues against a purely anionic subpicosecond solvation response. The existence of collective motion is not inconsistent with our suggestion of the role of the organic cation. Indeed, the motions of cations and anions must be correlated in order to ensure local electrical neutrality, a constraint imposed by the strong Coulombic interaction between ions. This is well documented by experimental measurements of radial distribution functions and by computer simulations.[60]

Finally, we have discussed a means of computing the reorganization energy due to intramolecular vibrations. The value obtained, 2068 cm^{-1}, is commensurate with that obtained from computing the reorganization energy from the zero-time spectra, 1870 ± 185 cm^{-1}, which speaks to the appropriateness of our method as well as to the robustness of the zero-time method.

Acknowledgment. We thank Ms. T. Fadeeva of Professor E. W. Castner, Jr.'s group for providing us with some initial viscosity measurements and Professor Castner for helpful conversations. Professors R. Richert, M. Maroncelli, and H. Weingärtner kindly provided preprints of their work. We also thank Mr. Jeffrey Crank for providing us with the [TEA$^+$][NTf$_2^-$] and Ms. Tessa Calhoun for collecting and analyzing the C153 spectra used in the intramolecular reorganization energy calculations. X.S. thanks NSF for support from grant CHE0303758.

References and Notes

(1) Wilkes, J. S.; Zaworotko, M. J. *J. Chem. Soc., Chem. Commun.* **1992**, 965.

(2) Adams, C. J.; Earle, M. J.; Roberts, G.; Seddon, K. R. *Chem. Commun.* **1998**, 2097.

(3) Earle, M. J.; McCormac, P. B.; Seddon, K. R. *Chem. Commun. (Cambridge)* **1998**, 2245.

(4) Dyson, P. J.; Ellis, D. J.; Parker, D. G.; Welton, T. *Chem. Commun. (Cambridge)* **1999**, 25.

(5) Leadbeater, N. E.; Torenius, H. M. *J. Org. Chem.* **2002**, *67*, 3145.

(6) Mann, B. E.; Guzman, M. H. *Inorg. Chim. Acta* **2002**, *330*, 143.

(7) Wasserscheid, P.; Keim, W. *Angew. Chem., Int. Ed.* **2000**, *39*, 3772.

(8) Reynolds, J. L.; Erdner, K. R.; Jones, P. B. *Org. Lett.* **2002**, *4*, 917.

(9) Welton, T. *Chem. Rev.* **1999**, *99*, 2071.

(10) Nara, S. J.; Harjani, J. R.; Salunkhe, M. M. *Tetrahedron Lett.* **2002**, *43*, 2979.

(11) Yao, Q. *Org. Lett.* **2002**, *4*, 2197.

(12) Fletcher, K. A.; Pandey, S.; Storey, I. K.; Hendricks, A. E.; Pandey, S. *Anal. Chim. Acta* **2002**, *453*, 89.

(13) Grodkowski, J.; Neta, P. *J. Phys. Chem. A* **2002**, *106*, 5468.

(14) Handy, S. T.; Zhang, X. *Org. Lett.* **2001**, *3*, 233.

(15) Huddleston, J. G.; Rogers, R. D. *Chem. Commun.* **1998**, 1765.

(16) Dai, S.; Ju, Y. H.; Barnes, C. E. *J. Chem. Soc., Dalton Trans.* **1999**, 1201.

(17) Carda-Broch, S.; Berthod, A.; Armstrong, D. W. *Anal. Bioanal. Chem.* **2003**, *375*, 191.

(18) Dickinson, V. E.; Williams, M. E.; Hendrickson, S. M.; Masui, H.; Murray, R. W. *J. Am. Chem. Soc.* **1999**, *121*, 613.

(19) Armstrong, D. W.; Zhang, L.-K.; He, L.; Gross, M. L. *Anal. Chem.* **2001**, *73*, 3679.

(20) Huppert, D.; Ittah, V.; Kosower, E. M. *Chem. Phys. Lett.* **1989**, *159*, 267.

(21) Ittah, V.; Huppert, D. *Chem. Phys. Lett.* **1990**, *173*, 496.

(22) Chapman, C. F.; Maroncelli, M. *J. Phys. Chem.* **1991**, *95*, 9095.

(23) Karmakar, R.; Samanta, A. *J. Phys. Chem. A* **2002**, *106*, 6670.

(24) Karmakar, R.; Samanta, A. *J. Phys. Chem. A* **2002**, *106*, 4447.

(25) Karmakar, B.; Samanta, A. *J. Phys. Chem. A* **2003**, *107*, 7340.

(26) Ingram, J. A.; Moog, R. S.; Ito, N.; Biswas, R.; Maroncelli, M. *J. Phys. Chem. B* **2003**, *107*, 5926.

(27) Ito, N.; Arzhantsev, S.; Maroncelli, M. *Chem. Phys. Lett.* **2004**, *396*, 83.

(28) Ito, N.; Arzhantsev, S.; Heitz, M.; Maroncelli, M. *J. Phys. Chem. B* **2004**, *108*, 5771.

(29) Arzhantsev, S.; Ito, N.; Heitz, M.; Maroncelli, M. *Chem. Phys. Lett.* **2003**, *381*, 278.

(30) Arzhantsev, S.; Hui, J.; Baker, G. A.; Naoki, I.; Maroncelli, M. "Solvation dynamics in ionic liquids, results from ps and fs emission spectroscopy."; Femtochemistry VII, Castleman, A. W., Ed.; Elsevier, 2005.

(31) Arzhantsev, S.; Hui, J.; Naoki, I.; Maroncelli, M. *Chem. Phys. Lett.*, in press.

(32) Hyun, B.-R.; Dzyuba, S. V.; Bartsch, R. A.; Quitevis, E. L. *J. Phys. Chem. A* **2002**, *106*, 7579.

(33) Giraud, G.; Gordon, C. M.; Dunkin, I. R.; Wynne, K. *J. Chem. Phys.* **2003**, *119*, 464.

(34) Cang, H.; Li, J.; Fayer, M. D. *J. Chem. Phys.* **2003**, *119*, 13017.

(35) Shirota, H.; Funston, A. M.; Wishart, J. F.; Castner, E. W., Jr. *J. Chem. Phys.* **2005**, *122*, 184512/1.

(36) Rajian, J. R.; Li, S.; Bartsch, R. A.; Quitevis, E. L. *Chem. Phys. Lett.* **2004**, *393*, 372.

(37) Shirota, H.; Castner, E. W., Jr. *J. Phys. Chem. A* **2005**, *109*, 9388.

(38) Weingartner, H.; Knocks, A.; Schrader, E.; Kaatze, U. *J. Phys. Chem. A* **2001**, *105*, 8646.

(39) Daguenet, C.; Dyson, P. J.; Krossing, I.; Oleinikova, A.; Slattery, J.; Wakai, C.; Weingartner, H. *J. Phys. Chem. B*, accepted.

(40) Ito, N.; Huang, W.; Richert, R. *J. Phys. Chem. B* **2006**, *110*, 4371.

(41) Chowdhury, P. K.; Halder, M.; Sanders, L.; Calhoun, T.; Anderson, J.; Armstrong, D. W.; Song, X.; Petrich, J. W. *J. Phys. Chem. B* **2004**, *108*, 10245.

(42) Fee, R. S.; Maroncelli, M. *Chem. Phys.* **1994**, *183*, 235.

(43) Baker, S. N.; Baker, G. A.; Munson, C. A.; Chen, F.; Bukowski, E. J.; Cartwright, A. N.; Bright, F. V. *Ind. Eng. Chem. Res.* **2003**, *42*, 6457.

(44) Jordanides, X. J.; Lang, M. J.; Song, X. Y.; Fleming, G. R. *J. Phys. Chem. B* **1999**, *103*, 7995.

(45) Mertz, E. L.; Tikhomirov, V. A.; Krishtalik, L. I. *J. Phys. Chem. A* **1997**, *101*, 3433.

(46) Kumar, P. V.; Maroncelli, M. *J. Chem. Phys.* **1995**, *103*, 3038.

(47) Song, X.; Chandler, D. *J. Chem. Phys.* **1998**, *108*, 2594.

(48) Song, X. *AIP Conf. Proc.* **1999**, *492*, 417.

(49) Zauhar, R. J.; Morgan, R. S. *J. Mol. Biol.* **1985**, *186*, 815.

(50) Zauhar, R. J.; Morgan, R. S. *J. Comput. Chem.* **1988**, *9*, 171.

(51) Yoon, B. J.; Lenhoff, A. M. *J. Comput. Chem.* **1990**, *11*, 1080.

(52) Davis, M. E.; McCammon, J. A. *Chem. Rev.* **1990**, *90*, 509.

(53) Bharadwaj, R.; Windemuth, A.; Sridharan, S.; Honig, B.; Nicholls, A. *J. Comput. Chem.* **1995**, *16*, 898.

(54) Pratt, L. R.; Tawa, G. J.; Hummer, G.; Garcia, A. E.; Corcelli, S. A. *Int. J. Quantum Chem.* **1997**, *64*, 121.

(55) Muhlpfordt, A.; Schanz, R.; Ernsting, N. P.; Farztdinov, V.; Grimme, S. *Phys. Chem. Chem. Phys.* **1999**, *1*, 3209.

(56) Margulis, C. J.; Stern, H. A.; Berne, B. J. *J. Phys. Chem. B* **2002**, *106*, 12017.

(57) Shim, Y.; Duan, J.; Choi, M. Y.; Kim, H. J. *J. Chem. Phys.* **2003**, *119*, 6411.

(58) Znamenskiy, V.; Kobrak, M. N. *J. Phys. Chem. B* **2004**, *108*, 1072.

(59) Kobrak, M. N.; Znamenskiy, V. *Chem. Phys. Lett.* **2004**, *395*, 127.

(60) Hansen, J. P.; McDonald, I. R. *Theory of simple liquids*, 2nd ed.; Academic: London, 1986.

(61) Bradaric, C. J.; Downard, A.; Kennedy, C.; Robertson, A.; Zhou, Y. *Green Chem.* **2003**, *5*, 143.

(62) Seddon, K. R.; Stark, A.; Torres, M.-J. Viscosity and density of 1-alkyl-3-methylimidazolium ionic liquids. *Clean Solvents: Alternative Media for Chemical Reactions and Processing*; ACS Symposium Series, Vol. 819; American Chemical Society: Washington, DC, 2002; p 34.